

ARTICLE

Multiscale Model Identifies Improved Schedule for Treatment of Acute Myeloid Leukemia *In Vitro* With the Mcl-1 Inhibitor AZD5991

Ardeshir Goliaei^{1,2}, Haley A. Woods³, Adriana E. Tron^{3,4}, Matthew A. Belmonte³, J. Paul Secrist³, Douglas Ferguson¹, Lisa Drew³, Adrian J. Fretland¹, Bree B. Aldridge^{5,6} and Francis D. Gibbons^{1,*}

Anticancer efficacy is driven not only by dose but also by frequency and duration of treatment. We describe a multiscale model combining cell cycle, cellular heterogeneity of B-cell lymphoma 2 family proteins, and pharmacology of AZD5991, a potent small-molecule inhibitor of myeloid cell leukemia 1 (Mcl-1). The model was calibrated using *in vitro* viability data for the MV-4-11 acute myeloid leukemia cell line under continuous incubation for 72 hours at concentrations of 0.03–30 μM . Using a virtual screen, we identified two schedules as having significantly different predicted efficacy and showed experimentally that a “short” schedule (treating cells for 6 of 24 hours) is significantly better able to maintain the rate of cell kill during treatment than a “long” schedule (18 of 24 hours). This work suggests that resistance can be driven by heterogeneity in protein expression of Mcl-1 alone without requiring mutation or resistant subclones and demonstrates the utility of mathematical models in efficiently identifying regimens for experimental exploration.

Study Highlights

WHAT IS THE CURRENT KNOWLEDGE ON THE TOPIC?

During the past few years, considerable progress has been made in the discovery of Mcl-1 inhibitors, with four compounds currently undergoing evaluation in phase I clinical trials. Studies *in vitro* have shown that the duration of treatment has a critical impact on overall cell viability. In addition, mouse xenograft studies have shown that tumor regression lasting some weeks can be achieved using a single dose or repeated doses delivered daily or weekly. However, the optimal administration schedule for Mcl-1 inhibitors (i.e., to maximize efficacy) is currently unknown.

WHAT QUESTION DID THIS STUDY ADDRESS?

This study investigates the concentration-time profile for the Mcl-1 inhibitor AZD5991 that is able to elicit maximum cell killing *in vitro*.

WHAT DOES THIS STUDY ADD TO OUR KNOWLEDGE?

Our study uses a multiscale mathematical model incorporating elements of Mcl-1 pharmacology, cell cycle, cell

division, and importantly, cellular heterogeneity to investigate and prioritize treatment schedules for experimental investigation. In the specific case of AZD5991, this study suggests that the repeated inhibition of Mcl-1 for a short period of time each cycle may be more efficacious for the longer term than inhibition during a longer portion of each cycle.

HOW MIGHT THIS CHANGE DRUG DISCOVERY, DEVELOPMENT, AND/OR THERAPEUTICS?

A critical aspect of drug discovery is to determine the dose and schedule that elicits the maximum intended effect with minimal toxicity. This information is needed to support the selection of a drug candidate and regulatory filing that precede clinical evaluation. The possibility of using a mathematical model to prioritize experiments for validation could significantly accelerate these late preclinical activities, enabling a better understanding of the impact of dose and schedule before initiating clinical trials.

Tumorigenesis and cancer progression depend on a variety of mechanisms, among which resistance to apoptosis (programmed cell death) has been identified as one of the hallmarks.^{1,2} Apoptosis occurs through two main pathways: (i) The extrinsic pathway, which is activated once a death ligand (e.g., TRAIL) interacts with a death receptor

or (ii) the intrinsic or mitochondrial pathway, which can be initiated by a variety of cytotoxic stimuli and proapoptotic molecules.³ The major event that follows activation of the intrinsic pathway is mitochondrial outer membrane permeabilization, as a result of which proteins that normally reside in the mitochondrial space (e.g., cytochrome-c, Smac/

¹Drug Metabolism and Pharmacokinetics (DMPK), Oncology R&D, AstraZeneca, Waltham, Massachusetts, USA; ²Novartis Institutes for Biomedical Research, Cambridge, Massachusetts, USA; ³Bioscience, Oncology R&D, AstraZeneca, Waltham, Massachusetts, USA; ⁴Agios Pharmaceuticals, Cambridge, Massachusetts, USA; ⁵Department of Molecular Biology and Microbiology, Tufts University School of Medicine, Boston, Massachusetts, USA; ⁶Department of Biomedical Engineering, Tufts University, Medford, Massachusetts, USA. *Correspondence: Francis D. Gibbons (frank.gibbons@astrazeneca.com)

Received: August 7, 2019; accepted: April 20, 2020. doi:10.1002/psp4.12552

DIABLO) translocate to the cytosol and initiate activation of caspases,⁴ an event that represents an irreversible commitment to apoptosis.

The B-cell lymphoma 2 (Bcl-2) family of proteins are major regulators of the intrinsic apoptotic pathway characterized by the presence of at least one of four Bcl-2 homology (BH) domains.⁵ They comprise several groups: (i) prosurvival proteins (Bcl-2, Bcl-XL, Bcl-W, Mcl-1, and Bfl1), (ii) multi-BH domain cell-death effector proteins (Bax, Bak, and Bok), and (iii) the BH3-only apoptosis initiator proteins (Bim, Puma, Noxa, and Bad). Interaction among Bcl-2 proteins involves binding of the BH3 domain of the proapoptotic protein to a groove on the surface of the prosurvival proteins. The relative expression of prodeath and prosurvival Bcl-2 proteins and their interaction with each other control commitment to apoptosis.⁶ (See ref. 7 for a useful introduction to this complex pathway.)

Maintenance of the balance between apoptosis and proliferation is crucial in hematological cells given their high turnover rate.⁸ The intrinsic apoptotic pathway is most commonly dysregulated in lymphoid malignancies⁹ through one of the following mechanisms: (i) Reduction in expression of the BH3-only proapoptotic proteins, (ii) loss of Bax and/or Bak, or (iii) enhancement of the expression of the prosurvival Bcl-2 proteins.

Among prosurvival Bcl-2 proteins, myeloid cell leukemia 1 (Mcl-1) is of particular interest given that its overexpression was found to promote the development of acute myeloid leukemia (AML),¹⁰ multiple myeloma¹¹ and other hematological malignancies.¹² AZD5991, a novel BH3 mimetic,^{13,14} is a selective Mcl-1 inhibitor that triggers mitochondrial outer membrane permeabilization and causes a potent and selective apoptotic response in multiple myeloma and AML cell lines *in vitro*. Administration of a single dose of AZD5991 has been shown to be sufficient to cause rapid tumor regression *in vivo* in multiple mouse xenograft models.¹⁴ Although regression is observed, tumors may regrow in the same site, indicating that a fraction of cancer cells too small to be detected immediately following treatment survived the treatment. Fractional kill of the cell population was also seen in cell viability studies *in vitro* in cell lines treated continuously during the course of 72 hours. Similar observations have been reported in cells treated with TRAIL.¹⁵ Interestingly, if the surviving population is treated once again after allowing for recovery, the same fractional killing is observed following another round of treatment with TRAIL.

A major challenge with anticancer therapies is to determine the optimal regimen, maximizing efficacy while minimizing toxicity. Although some approaches have been empirical (e.g., the “3 + 7” induction regimen used for AML¹⁶), others have applied optimal-control techniques.^{17,18} Such approaches tend to be phenotypic, focusing on efficacy and toxicity end points without offering much insight into the mechanism underlying the disease. A particular concern heard from clinicians is that drug-free intervals may offer a path for cancer cells to develop resistance.^{19,20}

We aimed to build a model to allow us to interrogate a wide range of schedules and identify those with predicted maximal longer term efficacy for further experimental exploration. Our goal was to triage potential schedules for

validation and then use the model to interrogate the differences to build hypotheses as to the underlying mechanisms. Taken together, our analyses suggest that studying the role of Mcl-1 protein, and its evolution under treatment, can shed light on the optimal choice of regimen.

MATERIAL AND METHODS

Multiscale systems pharmacology model

We developed a multiscale model using different techniques to describe the biology relevant at each scale (or “level”). At the foundation is the physicochemical model, which describes the pharmacology of the AZD5991 molecule and its interaction with molecules in the intrinsic apoptotic pathway. A step up from that is the cell cycle model, which operates at a phenotypic level rather than a molecular level. Finally, the agent-based model framework is used to bring in stochasticity in protein expression, enabling a collection of cells to be modeled for a timespan of several cell cycles. This approach has been used in the past to model the spatial heterogeneity of tumor cells, particularly in reference to “diffusibles”: primarily drug concentration and oxygen supply.^{21,22} Because our cells do not form a solid tumor but are suspended in liquid media *in vitro*, we assume that diffusion is not a limiting factor, and instead use the agent-based model as a framework on which to build a model of heterogeneity in protein expression within a population of genetically identical cells. Each agent of the agent-based model is running its own physicochemical and cell-cycle models based on the pharmacology of AZD5991 and behavior of the MV-4-11 cell line. These models are described in the **Supplementary Information** and the sections that follow.

Model development and calibration

In the **Supplemental Methods**, we discuss in more detail the construction of the physico-chemical, cell-cycle, and agent-based models as well as the *in vitro* cell culture and washout experiments. We provide more details on the inheritance rules for protein expression and how a distribution can “relax” to its initial form even when individual cells lack such a mechanism. We also define the “normalized slope” parameter, which we use to compare regimens, and the statistical test used to assess significance. We show how the model can recapitulate a wide range of phenotypic outcomes using only protein expression as input. Simulations are compared against not only MV-4-11 (an AML cell line) but also a range of multiple myeloma cell lines.

Description of training data by a multiscale model

To better understand the effect of scheduling in maximizing activity against cancer cells, we built a mathematical model to simulate the time course of cell survival at various concentrations. We calibrated this model against the experimental cell-kill curves under constant incubation to 72 hours. **Figure S3** illustrates how this model provides qualitative agreement with the data in a number of key areas. As highlighted in **Figure S3A**, the pharmacology of AZD5991 in AML cell lines exhibits a number of notable features. First, the rate of cell death is concentration

dependent and saturable; second, it is fractional; and third, it is biphasic. That it is concentration dependent is easily seen because as concentration increases, the rate of loss in viability increases. It is saturable because, beyond a certain concentration, that rate of loss no longer increases. By “fractional” we mean that the absolute rate of cell death depends on the number of cells remaining: When plotted on a log-linear scale, such behavior is a straight line. When we say that the loss in viability in a population of cells is biphasic, we simply mean that some cells die rapidly, whereas a smaller fraction manage to survive for a comparatively long time. In each of the two phases, the rate of cell kill is exponential (i.e., log-cell-kill is linear) in time, although clearly on a timescale that covers both phases, the effect will be non-linear. In certain cell lines, it appears that these persister cells may be regrowing (see **Figure S5A**, AMO-1 at 0.1 μM for an example). **Figure S1B** illustrates how our model can qualitatively capture most aspects of this cellular behavior.

Virtual washout screen and experimental validation

Once the multiscale model was in qualitative agreement with the *in vitro* viability experiments, a series of virtual washout screens was done to explore the effect of schedule differences in cell-kill profiles. We looked at incubation durations of various lengths, assuming a 24-hour treatment cycle because it fits the schedule of both drug discovery and clinical utility. We use a shorthand to describe the regimens: “6ON” refers to a schedule in which we incubate with drug for 6 hours and then wash out and incubate in drug-free medium for 18 hours, whereas “18ON” describes incubation with drug for 18 hours followed by wash out and drug-free incubation for 6 hours. Other regimens may be named by analogy, for example, 3ON, 12ON, etc. We examined a range of cycles with incubation period increasing in 3 hours increments from 3 to 21. We describe in the **Supplemental Methods** the design, execution, and statistical analysis of the experimental washout screens.

RESULTS

In these studies, we rely heavily on the concept of representative cell lines, by which we mean a pattern of protein expression that elicits a phenotypic response, such as being “sensitive” or “resistant” to treatment. We call them “representative” because they illustrate particular phenotypic responses on the spectrum of possibilities. (See **Figure S5** for experimental data and simulated profiles.)

Differential schedule sensitivity *in vitro*

Virtual schedule screening. Using a model enables us to rapidly screen many possible regimens. The *in vitro* doubling time of this model is around 40 hours, and because our model included cell cycle in a multiscale fashion, we could simulate durations long enough to see the effects of selective pressure on a heterogeneous population of cells over a few cell cycles.

We started by simulating a variety of experimentally tractable schedules (e.g., 3ON, 6ON, 12ON, 18ON), with the goal of predicting schedules that most effectively kill tumors by restraining their ability to develop resistance. **Figure 1**

shows simulated cell-kill curves during a 15-day period. As shown in **Figure 1a**, at sufficiently low drug concentrations (e.g., 1 arbitrary unit), there is no difference between 6ON and 18ON schedules; most cells grow and divide with no significant cell death. Also, at high concentrations (20 arbitrary units), there is no difference between schedules because the majority of cells die quickly. However, at intermediate concentrations (5 arbitrary units), the simulations suggest that 6ON can achieve more cell kill compared with a 18ON schedule during the same length of treatment (15 days). It does this by maintaining the cell-kill effect for multiple cycles, whereas on the 18ON schedule, this effect wears off.

Validation of schedule sensitivity. To validate this prediction, *in vitro* washout tests for the MV-4-11 cell line were performed for four 24-hour cycles (**Figure 1b**; described in detail in the **Supplementary Methods**). The major difference between schedules during this shorter duration, as predicted by modeling, is not in the final survival end point, but in the rate of cell kill and the extent of its conservation for repeated cycles of exposure to AZD5991. As predicted by the model (and shown in **Figure 1c**), the rate of cell kill during the “ON” phase is expected to diminish in the second cycle compared with the first on both schedules. Thereafter, it is expected to be largely maintained for successive cycles on both schedules; however, the relative magnitude of the loss in cell-kill rate is predicted greater for the 18ON than for the 6ON schedule. We assessed the experimental data using a linear mixed effect model (description, model code, and output in the **Supplementary Methods**). Comparing the effect on cell kill of both schedules and all four cycles, we found a significant ($P = 4.48 \times 10^{-7}$) effect of schedule on the initial slope, in which the initial value is approximately 0.035 hour^{-1} (for the “18ON” schedule) but is almost twice that (i.e., 0.060 hour^{-1}) on the 6ON schedule. This is visually evident in **Figure 1d** and expected from how the cell-kill slope is defined. From that initial value, the absolute decline is highly significant and similar for each subsequent cycle, in the range of $0.020\text{--}0.024 \text{ hour}^{-1}$ ($P = 6.17 \times 10^{-7}$, 9.74×10^{-7} , 2.41×10^{-5} for cycles 2, 3, and 4, respectively). This means that the slope for 18ON drops from 0.035 hour^{-1} to $0.011\text{--}0.015 \text{ hour}^{-1}$ (a drop of 57–68%), whereas for 6ON it drops from 0.06 hour^{-1} to $0.036\text{--}0.040 \text{ hour}^{-1}$ (a drop of 33–40%). In other words, the higher baseline of the 6ON schedule means that it suffers a smaller relative loss in its ability to maintain cell kill. There is a significant interaction ($P = 0.043$) only between schedule and cycle 2, which indicates that the change from cycle 1 to cycle 2 is similar in magnitude for both schedules and that (broadly speaking) both schedules maintain their respective new slope for successive cycles. This clearly shows that, although both schedules show an absolute loss in cell kill on the second and subsequent doses, the relative loss is significantly less with the 6ON schedule compared with 18ON. During the course of 15 days, the cumulative effects could be expected to lead to enhanced overall cell kill on the 6ON schedule compared with the 18ON schedule.

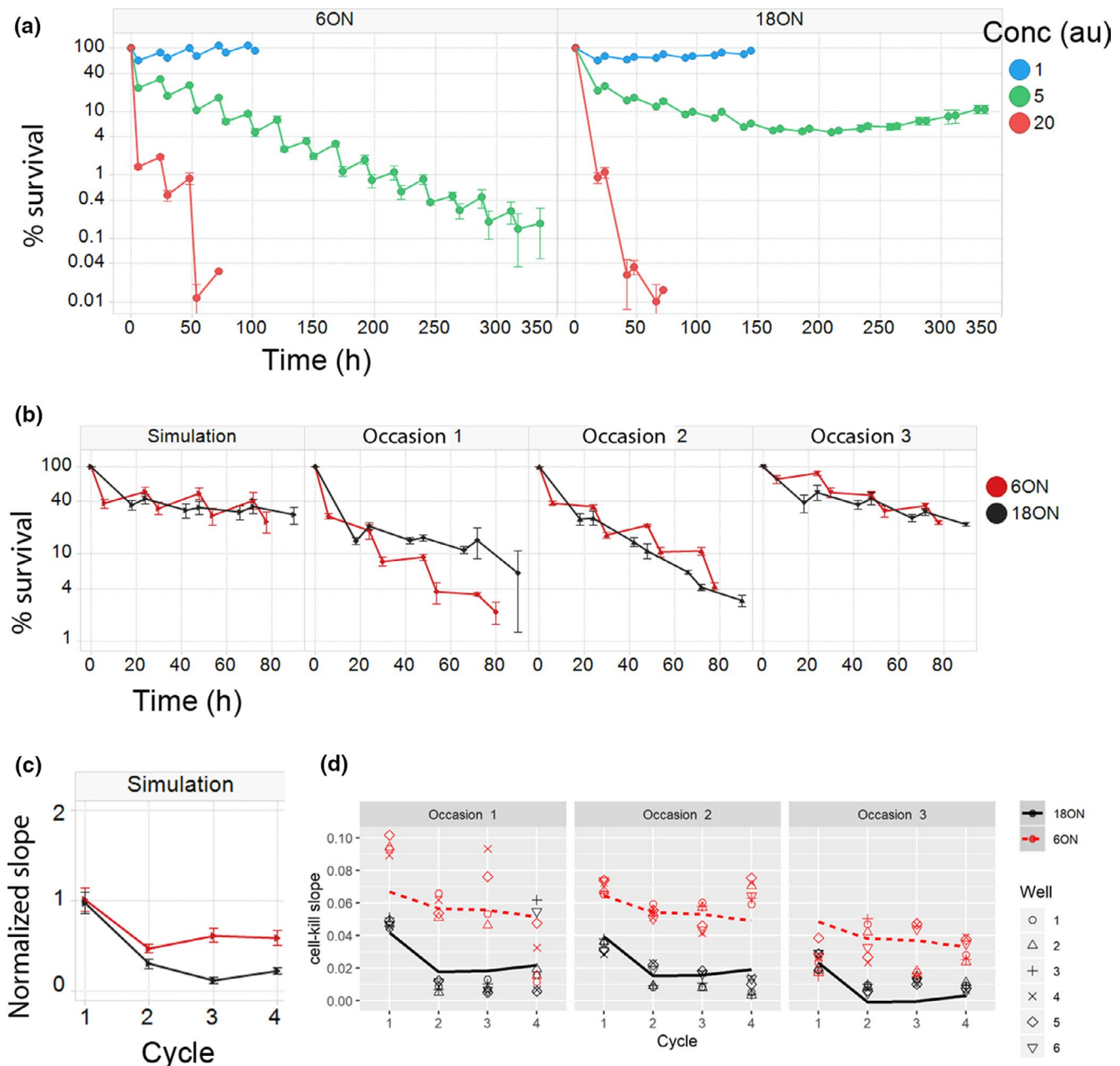


Figure 1 Schedules vary in their ability to maintain cell-kill rate; identified by virtual screen and validated *in vitro*. (a) Virtual *in vitro* washout studies compare cell survival on two schedules (6ON vs. 18ON) during 15 cycles of 24 hours. Mean \pm SD of three replicates, colors represent drug concentrations (arbitrary units). (b) Simulated survival shown alongside experimental biological replicates treated for four cycles (incubated at 100 nM AZD5991). Mean \pm SD of three technical replicates for each biological replicate. (c) Simulated slope of curve during "ON" portion of cycle, indicating rate of cell kill per unit time. Data are normalized against kill rate from cycle 1. (d) Slope of cell-kill curve from experimental replicates, showing data for each schedule as points and the linear mixed effect model overlaid as lines. See text for details and statistical analysis. 6ON, the regimen in which cells are incubated in AZD5991 for 6 hour, after which compound is washed off; the cycle repeats every 24 hour; 18ON, the regimen in which cells are incubated in AZD5991 for 18 hour, after which compound is washed off; the cycle repeats every; au, arbitrary units; Conc, concentration of AZD5991.

Selective pressure of the drug on Mcl-1 distribution. To explain the difference in observed outcomes from the two schedules, the simulated Mcl-1 expression in the surviving population were analyzed over time, as shown in **Figure 2**. On the 6ON schedule, the distribution of protein expression

remains mostly unchanged over time. This is consistent with the observation that each cycle shows the same rate of cell kill. Meanwhile, on the 18ON schedule, the distribution gets flatter and wider over time, with the mean tending toward increasing levels of Mcl-1 expression.

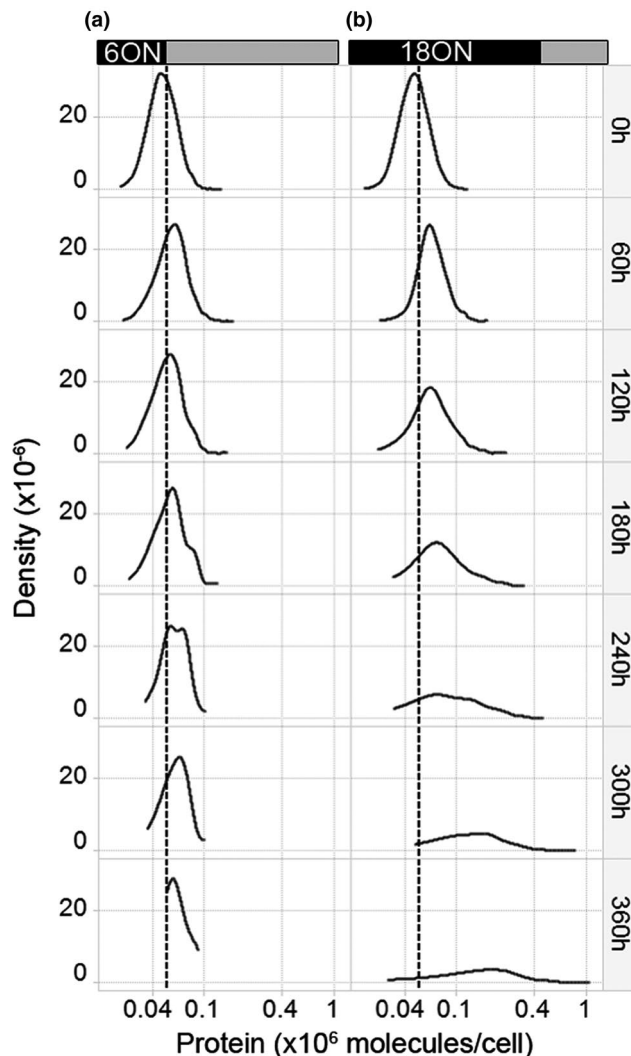


Figure 2 Overall distribution of protein expression may remain the same (“6ON”) or rapidly evolve (“18ON”) under constant incubation. The effect of two different schedules on the expression level of Mcl-1 of the survivors is shown as a probability density at intervals of 60 hours during the course of the 15-day virtual screen shown in **Figure 1**. (a) “6ON,” with short black and long gray bars indicating the short 6-hour duration of treatment during each 24-hour period. (b) 18ON, with long black and short gray bars indicating the long 18-hour duration of treatment during each 24-hour period. The average value of Mcl-1 (50,000 molecules/cell) of the founding population is shown as a vertical dashed line. 6ON, the regimen in which cells are incubated in AZD5991 for 6 hour, after which compound is washed off; the cycle repeats every 24 hours; 18ON, the regimen in which cells are incubated in AZD5991 for 18 hour, after which compound is washed off; the cycle repeats every; au, arbitrary units.

Sensitivity analysis. As shown in **Figure S5C,D**, several cell lines show an initial response followed by regrowth during the course of 72 hours of treatment. To study the effects of scheduling on different cell lines, we focused on two representative cell lines: Sensitive and resistant. Their differences are highlighted in **Figure 3**. We define a hypothetical cell line as “sensitive” when all drug concentrations tested result in complete cell kill after

a 72-hour treatment period (**Figure 3b**). By contrast, a hypothetical cell line is called “resistant” if even a high concentration of the drug was not able to eliminate the cells and a survivor population emerges during 72 hours of continuous treatment (**Figure 3e**). As expected from a biological perspective, a sensitive cell line will have lower average levels of Mcl-1 than a resistant cell line (compare **Figure 3a** and **Figure 3d**). Once these two representative cell lines were selected, we evaluated whether differential sensitivity on schedule has any impact on cell killing. As shown in **Figure 3c**, no benefit from scheduling was demonstrated in the sensitive cell line as all schedules tested resulted in complete cell kill. However, in a more resistant cell line (**Figure 3f**), there is a potential benefit from using the 6ON schedule compared with the 18ON schedule as the former achieves complete cell kill, whereas the latter develops resistance at the concentrations tested.

Resensitization of a survivor population. Because nongenetic markers of sensitivity, such as Mcl-1 protein expression, can be labile for a short timescale,¹⁵ an important follow-on question in designing a treatment strategy is the following: What is the relaxation time? In other words, once a state of increased protein expression has been attained and drug treatment is stopped, how long does it take for the distribution of protein expression to return to the original baseline condition? Our model does not contain an explicit “relaxation” process; rather, it arises through the process of population turnover as cells with higher expression are replaced by those with expression matching the “founding population” distribution. The current model allowed us to mechanistically study this question based on the distribution of Mcl-1 protein expression and its movement over time under the effect of the drug. **Figure 4a** shows the predicted distribution of Mcl-1 expression in a simulated experiment in which cells are first incubated for 72 hours, after which time the drug is withdrawn. At first, during the incubation phase, starting after 24 hours, there is a rightward shift in expression (as shown in **Figure 3**), so that by 72 hours, the distribution of Mcl-1 has shifted significantly toward higher values. At this point, the drug is withdrawn, and gradually the distribution returns to its baseline. The process is largely complete by 120 hours. A more detailed look at Mcl-1 protein distribution in the time interval between 96 and 120 hours is shown in **Figure 4b**.

DISCUSSION

In this study, we modeled resistance in cancer cells to treatment with a proapoptotic compound as a shift in the distribution of protein expression. Drawing on the evolutionary similarities between mitochondria and bacteria,²³ we reasoned that a model considering only binding kinetics, cellular heterogeneity, and cell proliferation could describe many phenomena observed *in vitro* with an agent that induces the intrinsic mitochondrial apoptotic pathway, e.g., fractional cell kill, steep dose response, and heterogeneity-based resistance. After model calibration, we identified schedules with differential predicted activity

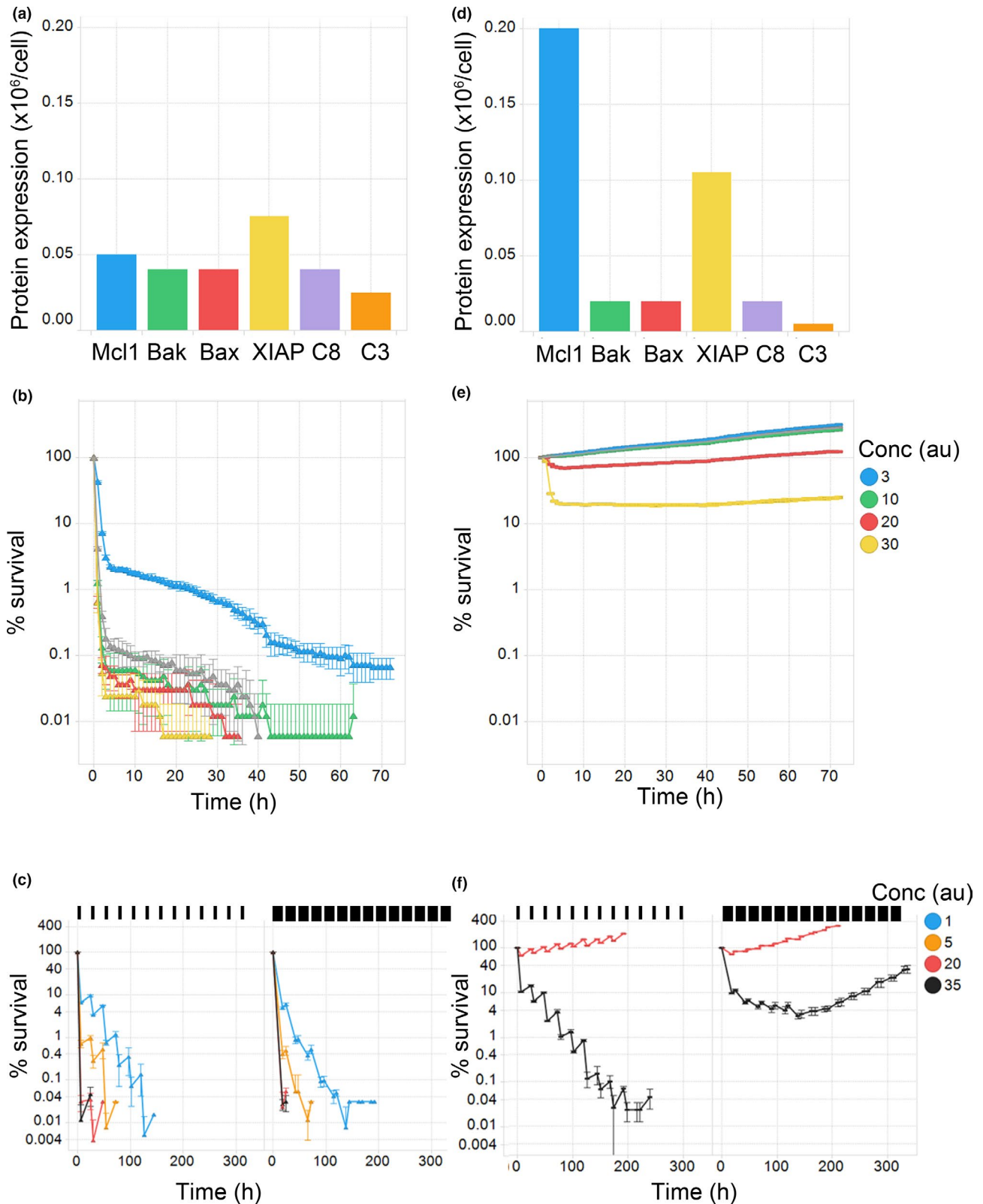


Figure 3 Two representative cell lines: one “sensitive” and the other “resistant.” (a) The average abundance (no. molecules/cell) of Mcl-1, Bak, Bax, XIAP, C8, and C3 in the founding population of a “sensitive” representative cell line. (b) Simulated average survival for sensitive cell (mean \pm SD of three virtual replicates). (c) Virtual screen results for two schedules: 6ON and 18ON. Bars at the top represent the schedule (black is “on,” white is “off”). Concentrations in arbitrary units (au). (d–f) As in a–c, but for a “resistant” representative cell line. Conc, concentration of AZD5991.

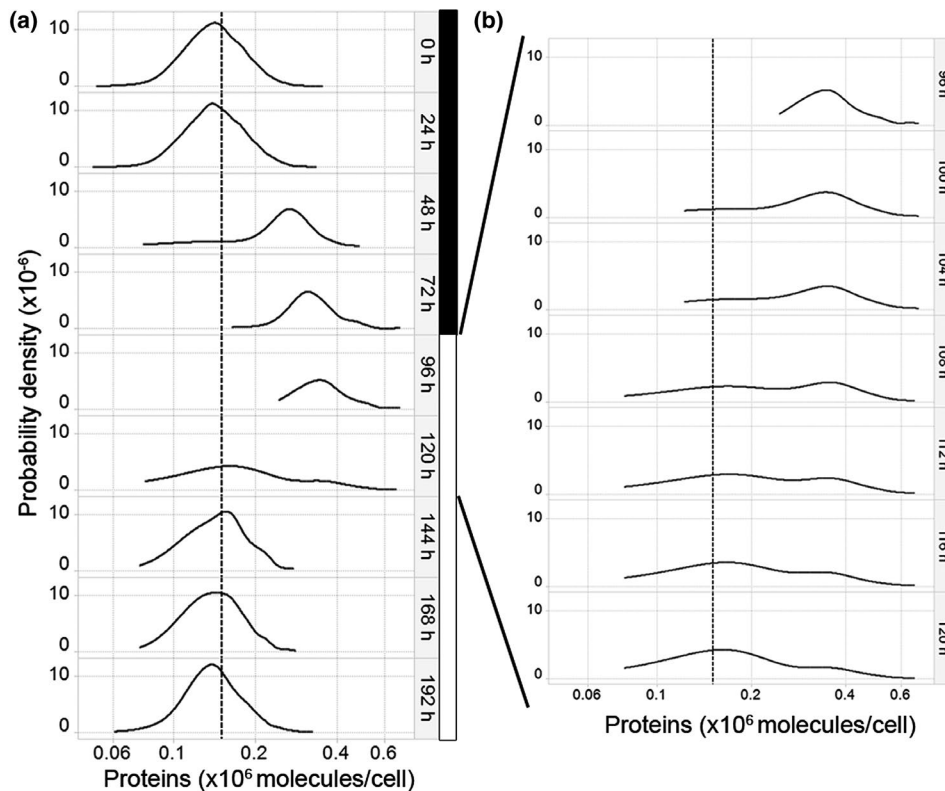


Figure 4 Reversion of protein distribution to baseline following evolution for 72 hours. (a) Predicted evolution of the probability density for the Mcl-1 protein in a resistant model when incubated at constant drug concentration for 72 hours (represented by black vertical bar) and then washed out (represented by white vertical bar) and followed to 192 hours. The average value of the distribution (150,000 molecules/cell) in the surviving population is represented as dashed line. (b) The same data but focusing with more temporal granularity on the interval 96–120 hours, during which the cells begin to show regression to the founding distribution.

and showed experimentally that indeed they have a significantly differential impact on the ability of AZD5991 to maintain its cell killing ability. Similar to all models, ours makes a number of simplifications, not the least of which are assumptions around the role of Mcl-1 protein levels in defining sensitivity to AZD5991 and identical binding kinetics of AZD5991 to Mcl-1 regardless of proteins already associated with Mcl-1. The apoptotic pathway is complex, encompassing numerous proteins with various levels of binding specificity toward their potential partners. Because the Mcl-1 expression level has been shown to drive resistance to cell-death agents,²⁴ we focus on the role of this protein in particular in driving resistance to a cell-death agent, although certainly others will also play a role.

Resistance to treatment is a concern across many fields. Bacterial resistance^{25,26} is often described using the concepts of “sensitive,” “resistant,” and “quiescent” populations without further explanation at the molecular level of the processes that give rise to these phenotypes. In oncology, it is commonly understood in terms of discrete mutations conferring a reduced response to particular targeted treatments by inhibiting binding to the target domain, causing constitutive (i.e., ligand independent) activation of the target pathway or other means.²⁷

However, recent work on resistance in bacterial populations has shown that it is not necessary to invoke arbitrary

distinctions between sensitive and resistant cell populations.^{23,28} Rather, a combination of chemical binding kinetics and cellular heterogeneity can explain observations such as a postantibiotic effect (duration of response after drug has washed out) or inoculum effect (fractional killing in larger populations) among others. Mitochondria were once free-living organisms that became symbiotically incorporated into eukaryotic cells in the distant past yet retain their own genomes and ribosomes and show strong genomic similarity to intracellular bacteria.^{29,30} Furthermore, it has been shown experimentally that stochastic fluctuations in protein expression can yield rare cells in an otherwise genetically identical population, which are rendered resistant to treatment with anticancer drugs.³¹ The work of ref. 31 shows that, at least for melanoma treated with kinase inhibitors, mutation is not the only pathway to resistance and that certain rare cells can become transiently preresistant, with further treatment initiating a kind of cellular reprogramming that leads to what the authors term “burn in” of a resistant phenotype. Although they do not speculate as to the mechanism of burn in, the authors allude to the idea that brief drug exposure might be insufficient for the process to complete, allowing cells to revert to the drug-sensitive state. We sought to bring together these three ideas: Mitochondria as bacterial analogs, cell death limited by chemical

kinetics, and nongenetic resistance mediated through exposure to anticancer agents. Given that cell-death agents such as AZD5991 target the intrinsic mitochondrial apoptotic pathway, we reasoned that similar methods might apply to cancer cells dependent on BH3 family proteins.

We investigated whether fractional killing could be driven by cellular heterogeneity in protein abundance as distinct from genetic alterations.³² In human cells, this abundance follows a long-tailed, right-skewed distribution,^{33,34} commonly modeled as log-normal: A small number of cells (in the tail) display expression of specific proteins at a much higher level than the bulk of the population, allowing them to respond differently to treatment, ultimately leading to a phenotypically resistant population. To our knowledge, it has not yet been established how plastic this expression might be. It has been shown that protein half-life follows a wide distribution centered (in log-space) around approximately 100 hours, with a tendency toward longer stability in the mitochondria compared with other cellular compartments,³⁵ but to alter expression levels would require a change in either synthesis or degradation rates, neither of which is well characterized as yet. With a half-life on the order of an hour or so, Mcl-1 is anomalous even among Bcl-2 family proteins³⁶ and might be more susceptible than most to rapid changes in protein expression. In our model, the abundance of proteins in a given cell is fixed at the time of birth; we do not include a means by which cells can alter their protein expression during the cell cycle. Changes in the overall population distribution occur because of the “inheritance” rules, which govern the determination of protein expression at the time of cell division.

Importantly, and in line with the work of Shaffer *et al.*,³¹ we never found it necessary to assume two distinct *a priori* populations (sensitive and resistant). Furthermore, we did not find it necessary to assume a separate resistance mechanism, such as through a compensating pathway. Rather, we found that a resistant phenotype emerges following drug treatment through the combination of survival of resistant, high-expressing cells and stochastic inheritance of that same resistant high-expressing phenotype by the daughter cells. Higher expression increases the chance of survival, but inheritance of higher expression is stochastic, with a finite chance the daughter cells may have expression either lower or higher than the parental cell. Over successive generations, this will tend to widen the distribution of Mcl-1 expression within a population for which the selective pressure is mostly present (e.g., 18ON; see **Figure 2**). Yet, because the number of cells has declined over time, the distribution must simultaneously become flatter. Because cells with higher Mcl-1 expression are less sensitive, this is consistent with reduced cell kill on successive cycles. This suggests a mechanism by which cell populations may rapidly become resistant to therapy under near-constant pressure. Although we did not directly measure Mcl-1 expression in these studies, the role of increased Mcl-1 protein expression as a means of resistance to anticancer therapy is well supported.^{37,38} Certainly there could be other explanations, such as a change in the affinity of the binding partners (e.g., Bim). However, our goal here was to provide a model for how such nongenetic resistance

could arise and be maintained through little more than the known heterogeneity of cells and simple rules around inheritance upon cell division, and furthermore to illustrate how such a model could enable rapid triage of possible dose regimens for experimental validation.

According to model predictions, the time it takes for a resistant population to revert back to a population similar to the initial population is about one cell cycle (40 hours; **Figure 4b**). This observation is to be expected from the assumptions made in the model. We assumed that Mcl-1 expression levels in a given cell do not change over time (production and synthesis rates are constant at all times). Because the tumor models used in this work exhibit rapid doubling times *in vitro* (e.g., the 40 hours we use in this work) and *in vivo* (clinical doubling AML may be as short as 3 days³⁹), the lack of mechanism to alter expression during the lifetime of a single cell does not seem to us a severe limitation. As a result, founder cells start with a particular protein level at birth. However, upon division, the daughter cells have characteristics that are determined both by parents (as baseline for expression) and environment (inheritance rules depend on presence of drug). Consequently, a resistant population that is generated by selective drug pressure needs to be replaced because members do not evolve. When that pressure is removed, their replacement by daughter cells will cause the distribution of protein expression to drift back to the baseline “founder” distribution. In this way, the relaxation time is an emergent property of the cell cycle time and degree of change from the founding distribution. It is apparent that on a 24-hour cycle, once the resistant phenotype emerges, there will never be sufficient time for protein expression to relax, highlighting the importance (under our model) of avoiding it in the first place through short exposure.

The scope of this work has been limited to *in vitro* systems and to the timescale of a few days, over which such systems are viable. An ideal outcome of our experimental work would have been to show a durable, statistically significant interaction between schedule and cycle because that would clearly indicate increased divergence between the efficacy of the two schedules. What we have found is that there is a statistically significant difference between the two schedules on the second dose, where the 6ON schedule shows a relatively smaller loss in cell killing than the 18ON schedule and that this difference is maintained (but not augmented) on successive cycles. This finding supports our hypothesis, although further work is needed for full validation. A logical next step would be to investigate whether such differences also hold *in vivo*, enabling studies to run to a longer timescale. This would likely need to be carried out in disseminated models rather than traditional subcutaneous xenograft models because the physico-chemical properties required of a compound to disrupt the protein–protein interactions can also lead to long retention time in solid tumors, which would make it hard to test the hypothesis. The shorter duration (6 hours) could be achieved through intravenous infusion of a short half-life compound (so that exposure does not persist much beyond the end of infusion). Although ref. 14 does not quote a half-life, it is readily seen from **Figure S6C** of that article that the plasma half-life is a matter of hours, which makes

AZD5991 a suitable molecule to test the 6ON regimen. Other Mcl-1 inhibitors⁴⁰ can be delivered orally with half-life in excess of 12 hours. In clinical situations where maximal control of duration and degree of exposure is required, intravenous administration is routine. Infusions are also possible in rodents⁴¹ using commercially available solutions.

In summary, this study of the role of scheduling in BH3-mimetic induced cancer cell death provides a novel framework on which to build understanding of fractional cell killing of cancer cells *in vitro* when treated with an Mcl-1 inhibitor. It may be applied to other targets in the intrinsic apoptosis pathway, such as Bcl-2 and Bcl-xL. Specifically, after building a model including cell cycle, the intrinsic apoptotic pathway, drug pharmacology, and reasonable assumptions about how protein expression is inherited across generations, we identified two schedules showing differential cell kill rates. A linear mixed effects analysis of three separate experiments, which show statistically significant differences in retention of cell kill rates over time, provided supporting evidence for these counterintuitive predictions. Not only were these scheduling predictions first made using the model but also once validated, the model provided a platform on which to interrogate and build hypotheses for mechanisms underlying these observations. Together, this study highlights the value of mechanistic multiscale models in the discovery of optimal regimens for control of resistance. These findings enhance our understanding of how best to use BH3 mimetics, in particular how scheduling can affect the emergence of resistance in cancer cells as a consequence of selection within a heterogeneous population. To the best of our knowledge, this is the first model to incorporate systems pharmacology of an Mcl-1 inhibitor into the intrinsic apoptotic pathway.

Supporting Information. Supplementary information accompanies this paper on the *CPT: Pharmacometrics & Systems Pharmacology* website (www.psp-journal.com).

Acknowledgments. F.D.G. thanks Harish Shankaran for first inspiring him to think about the similarities between bacteria and mitochondria. The authors acknowledge the assistance of Patrick Mitchell in troubleshooting aspects of the linear mixed effects analysis. A.G.'s postdoctoral fellowship was funded by AstraZeneca's Innovative Medicines and Early Development (IMED) postdoctoral program.

Funding. This work was funded by AstraZeneca. B.B.A. was supported by an National Institutes of Health Director's New Innovator Award (1DP2LM011952).

Conflict of Interest. H.A.W., A.E.T., D.F., L.D., A.F., and F.D.G. are current employees and/or shareholders of AstraZeneca. All other authors declared no competing interests for this work.

Author Contributions. A.G., F.D.G., B.B.A., and A.E.T. wrote the manuscript. A.G., F.D.G., A.E.T., and B.B.A. designed the research. A.G., F.D.G., H.A.W., M.A.B., and A.E.T. performed the research. F.D.G., A.G., B.B.A., D.F., L.D., and A.J.F. analyzed the data. A.G. and J.P.S. contributed new reagents/analytical tools.

1. Hanahan, D. & Weinberg, R.A. Hallmarks of cancer: the next generation. *Cell* **144**, 646–674 (2011).
2. Hanahan, D. & Weinberg, R.A. The hallmarks of cancer. *Cell* **100**, 57–70 (2000).
3. Elmore, S. Apoptosis: a review of programmed cell death. *Toxicol. Pathol.* **35**, 495–516 (2007).
4. Fulda, S. & Debatin, K.-M. Extrinsic versus intrinsic apoptosis pathways in anticancer chemotherapy. *Oncogene* **25**, 4798–4811 (2006).
5. Czabotar, P.E., Lessene, G., Strasser, A. & Adams, J.M. Control of apoptosis by the BCL-2 protein family: implications for physiology and therapy. *Nat. Rev. Mol. Cell Biol.* **15**, 49–63 (2013).
6. Petros, A.M. *et al.* Rationale for Bcl-X_L/Bad peptide complex formation from structure, mutagenesis, and biophysical studies. *Protein Sci.* **9**, 2528–2534 (2000).
7. Haplo, L., Strasser, A. & Cory, S. BH3-only proteins in apoptosis at a glance. *J. Cell Sci.* **125**, 1081–1087 (2012).
8. Zaman, S., Wang, R. & Gandhi, V. Targeting the apoptosis pathway in hematologic malignancies. *Leuk. Lymphoma* **55**, 1980–1992 (2014).
9. Anderson, M.A., Huang, D. & Roberts, A. Targeting BCL2 for the treatment of lymphoid malignancies. *Semin. Hematol.* **51**, 219–227 (2014).
10. Glaser, S.P. *et al.* Anti-apoptotic Mcl-1 is essential for the development and sustained growth of acute myeloid leukemia. *Genes Dev.* **26**, 120–125 (2012).
11. Gong, J.-N. *et al.* Hierarchy for targeting prosurvival BCL2 family proteins in multiple myeloma: pivotal role of MCL1. *Blood* **128**, 1834–1844 (2016).
12. Powell, J.A., Lewis, A.C. & Pitson, S.M. The MCL-1 inhibitor S63845: an exciting new addition to the armoury of anti-cancer agents. *J. Xiangya Med.* **2**, 53 (2017).
13. Billard, C. BH3 mimetics: status of the field and new developments. *Mol. Cancer Ther.* **12**, 1691–1700 (2013).
14. Tron, A.E. *et al.* Discovery of Mcl-1-specific inhibitor AZD5991 and preclinical activity in multiple myeloma and acute myeloid leukemia. *Nat. Commun.* **9**, 5341 (2018).
15. Roux, J. *et al.* Fractional killing arises from cell-to-cell variability in overcoming a caspase activity threshold. *Mol. Syst. Biol.* **11**, 803 (2015).
16. Tallman, M.S., Gilliland, D.G. & Rowe, J.M. Review in translational hematology drug therapy for acute myeloid leukemia. *Drug Ther.* **106**, 1154–1163 (2005).
17. Parker, R.S. & Clermont, G. Systems engineering medicine: Engineering the inflammation response to infectious and traumatic challenges. *J. R. Soc. Interface* **7**, 989–1013 (2010).
18. Panetta, J.C. & Fister, K.R. Optimal control applied to competing chemotherapeutic cell-kill strategies. *SIAM J. Appl. Math.* **63**, 1954–1971 (2003).
19. Das Thakur, M. *et al.* Modelling vemurafenib resistance in melanoma reveals a strategy to forestall drug resistance. *Nature* **494**, 251–255 (2013).
20. De Souza, R., Zahedi, P., Badame, R.M., Allen, C. & Piquette-Miller, M. Chemotherapy dosing schedule influences drug resistance development in ovarian cancer. *Mol. Cancer Ther.* **10**, 1289–1299 (2011).
21. Cosgrove, J. *et al.* Agent-based modeling in systems. *Pharmacology* **4**, 615–629 (2015).
22. Wang, Z., Zhang, L., Sagotsky, J. & Deisboeck, T.S. Simulating non-small cell lung cancer with a multiscale agent-based model. *Theor. Biol. Med. Model.* **4**, 50 (2007).
23. Abel zur Wiesch, P. *et al.* Classic reaction kinetics can explain complex patterns of antibiotic action. *Sci. Transl. Med.* **7**, 287ra73 (2015).
24. Choudhary, G.S. *et al.* MCL-1 and BCL-xL-dependent resistance to the BCL-2 inhibitor ABT-199 can be overcome by preventing PI3K/AKT/mTOR activation in lymphoid malignancies. *Cell Death Dis.* **6**, e1593 (2015).
25. Nielsen, E.I. & Friberg, L.E. Pharmacokinetic-pharmacodynamic modeling of antibacterial drugs. *Pharmacol. Rev.* **65**, 1053–1090 (2013).
26. Park, K. A Review of modeling approaches to predict drug response in clinical oncology. *Yonsei Med. J.* **58**, 1–8 (2017).
27. Iranzo, J., Martincorena, I. & Koonin, E.V. Cancer-mutation network and the number and specificity of driver mutations. *Proc. Natl. Acad. Sci. U. S. A.* **115**, E6010–E6019 (2018).
28. Walkup, G.K. *et al.* Translating slow-binding inhibition kinetics into cellular and in vivo effects. *Nat. Chem. Biol.* **11**, 416–423 (2015).
29. Margulis, L. *Origin of Eukaryotic Cells* (Yale University Press, New Haven, CT, 1970).
30. Gray, M.W. Mitochondrial evolution. *Cold Spring Harb Perspect Biol.* **4**, a011403 (2012).
31. Shaffer, S.M. *et al.* Rare cell variability and drug-induced reprogramming as a mode of cancer drug resistance. *Nature* **546**, 431–435 (2017).
32. Brock, A., Chang, H. & Huang, S. Non-genetic heterogeneity—a mutation-independent driving force for the somatic evolution of tumours. *Nat. Rev. Genet.* **10**, 336–342 (2009).
33. Cohen, A.A. *et al.* Protein dynamics in individual human cells: experiment and theory. *PLoS One* **4**, e4901 (2009).
34. Sigal, A. *et al.* Variability and memory of protein levels in human cells. *Nature* **444**, 643–646 (2006).
35. Mathieson, T. *et al.* Systematic analysis of protein turnover in primary cells. *Nat. Commun.* **9**, 1–10 (2018).
36. Stewart, D.P. *et al.* Ubiquitin-independent degradation of antiapoptotic MCL-1. *Mol. Cell Biol.* **30**, 3099–3110 (2010).

37. Tahir, S.K. *et al.* Potential mechanisms of resistance to venetoclax and strategies to circumvent it. *BMC Cancer* **17**, 1–10 (2017).
38. Mckee, C.S., Hill, D.S., Redfern, C.P.F., Armstrong, J.L. & Lovat, P.E. Oncogenic BRAF signalling increases Mcl-1 expression in cutaneous metastatic melanoma. *Exp. Dermatol.* **22**, 767–769 (2013).
39. Bokhari, S.A.J. *et al.* Cell cycle parameters as biological predictors of prognosis in AML: a review and update of cell cycle kinetics and remission induction/duration in acute leukemia. *Leuk. Lymphoma* **6**, 197–207 (1992).
40. Caenepeel, S. *et al.* AMG 176, a selective MCL1 inhibitor, is effective in hematologic cancer models alone and in combination with established therapies. *Cancer Discov.* **1582** (2018). <https://doi.org/10.1158/2159-8290.CD-18-0387>
41. Nolan, T.E. & Klein, H.J. Methods in vascular infusion biotechnology in research with rodents. *ILAR J.* **43**, 175–182 (2002).

© 2020 The Authors *CPT: Pharmacometrics & Systems Pharmacology* published by Wiley Periodicals LLC. on behalf of the American Society for Clinical Pharmacology and Therapeutics. This is an open access article under the terms of the Creative Commons Attribution-NonCommercial-NoDerivs License, which permits use and distribution in any medium, provided the original work is properly cited, the use is non-commercial and no modifications or adaptations are made.